1st TMS/ABM International Materials Congress
TMS CO-ORGANIZADOR
ANAIS PROCEEDINGS
ISSN 1516-392X

ATOMISTIC MODELLING OF SHOCK LOAD IN NANOPHASE ALUMINUM NITRIDE CERAMICS

Paulo S. Branicio* and David J. Srolovitz*

Large scale molecular-dynamics simulations of plane shock loading in nanophase aluminum nitride are performed to reveal the interplay between shock-induced compaction, structural phase transformation and plastic deformation. The shock profile is calculated for a wide range of particle velocity from 0.2 km/s to 4 km/s. The calculated Hugoniot curves agree well with the experimental one. For lower particle velocity, below 0.8 km/s a single elastic wave is generated. For intermediate particle velocity, between 0.8 km/s and 4 km/s the generated shock wave splits into an elastic precursor and a wurtzite-to-rocksalt structural transformation wave. For particle velocities greater than 4 km/s a single overdriven transformation shock wave is generated above the longitudinal sound speed. These simulation results provide a microscopic view of the dynamic effects of shock impact on single crystal and nanophase high-strength ceramics.

Keywords: high strength ceramics, large scale molecular dynamics, shock load

Meeting: First TMS-ABM International Materials Congress
Proceedings Title: Dynamic Behavior of Materials
Included Symposia: Dynamic Behavior of Materials

*Materials Theory and Simulation Laboratory
Institute of High Performance Computing, A*STAR
1 Fusionopolis Way, 16-16, Connexis, 138632, Singapore

INTRODUCTION

One of the challenges in the field of shock wave loading is the description of shock effects in high strength ceramics. That is a crucial ingredient to potential application of these materials as coatings in light weight armor designs. The literature of experimental studies of these ceramics is extensive and includes shock experiments on several materials such as Al_2O_3, B_4C, and AlN[1-8].

In this work we examine the effects of strong plane shock waves on high strength AlN ceramics using million atoms MD simulations. To model AlN atomic interactions we use a many body potential that enables the calculation of the Hugoniot and the shock wave profile as well as the mechanisms of shear stress relaxation. The focus is set on the microscopic description of the nucleation and evolution of multi-shock wave structures at very high loadings.

METHODOLOGY

The system simulated is an AlN monocrystal slab with 15 x 15 x 200 nm^3 approximate dimensions and around 4 million atoms. The long z direction is aligned with the impact direction to let the shock waves develop for at least 15 ps. Before impact, the crystalline structure of the target material is wurtzite. The slab is oriented in such a way that the *z*-axis, chosen as the impact direction, is parallel to the [0001]. Periodic boundary conditions are imposed in the *x* and *y* directions. Free surfaces surround the system in the *z* direction. The particle velocity (u_p), which here is exactly the impact velocity, is in the range 0.2 - 5 km/s, accessing all shock wave regimes and shock pressures exceeding 150 GPa. The million equations of motion are numerically integrated at each time step of 1.5 fs. The plane impact simulation was performed in the reversed geometry with the system target initially set with the chosen impact velocity hitting the piston at a fixed position. The piston chosen is a hard wall which elastically bounces any particle hitting the piston surface, making the particle velocity of the slower shock wave equal to the impact velocity. Properties are calculated along the system in the impact z direction. Bins 5 Å wide are used to average local quantities and quantify the shock profile and the materials response.

The forces between atoms in the AlN slab are calculated from a many-body interatomic potential, which is validated by experimental results on lattice constants, elastic moduli, cohesive energy, and melting temperature.[9] A more stringent validation is provided by the wurtzite-to-rocksalt structural phase transition in AlN. High-pressure experiments reveal that this transformation occurs at ~20 GPa[7] and the calculated value is 25 GPa. This potential has been used succesfully to describe shock induced fracture in simulations of projectile impacts on AlN.[10, 11] The collisions with the piston are elastically therefore there is no interaction between the slabs and the piston.

RESULTS AND DISCUSSION

We have found three regimes for the shock response from the simulations which agree reasonably well with the experiments. The shock Hugoniot curves for simulations with T = 10 K and T = 300 K are shown in Fig. 1, which plot the calculated shock velocities against the particle velocities. The calculated results are compared with the experimental result of Mashima *et al.*[7] For particle velocities below v_p = 0.8 km/s the simulation shows only the presence of an elastic shock wave

which propagates with roughly constant velocity in the wurtzite phase. Experimentally at low particle velocities up to v_p = 0.6 km/s only an elastic wave is generated. What is in excellent agreement with our simulation result. However in a short range of velocities, from v_p = 0.6 km/s to v_p = 1 km/s, experiments show an intermediate shock wave which is associated with induced plastic deformations in the sample.[7] In our simulations we have not found the presence of plastic deformations and a shock wave associated with them. We believe this variance of results is related with the difference in systems used. We performed the simulations on defect free monocrystal wurtzite AlN while experiments are performed with polycrystalline samples. We do however expect to find an intermediate plastic deformation if a nano polycrystalline system is used instead. The simulation results in Fig. 1 indicate that above v_p = 0.8 km/s a structural phase transition shock wave develops inside the system and propagates with an increasing speed for higher v_p. Experimentally the transformation wave is detected for particle velocities above v_p = 1 km/s and also propagates with increasing speed for stronger shocks loads. Despite the differences in system geometry and crystal structures the simulation results agree reasonably well with the experimental Hugoniot. For particle velocities above v_p = 3.5 km/s the structural phase transition wave overlap with the elastic wave forming a single overdriven wave. The results indicate that no plastic wave is induced directly by compression before the transformation takes place.

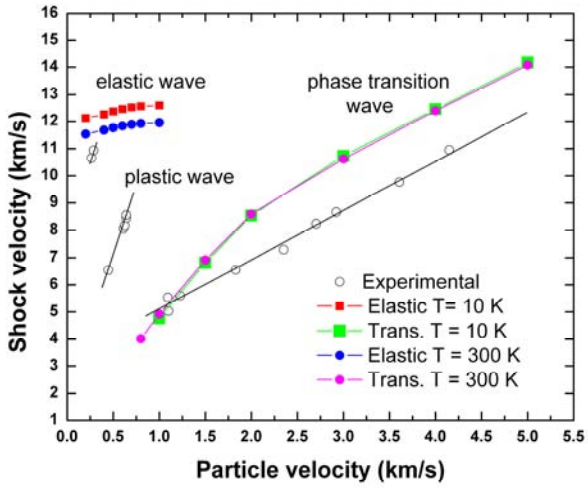

Fig. 1 AlN shock Hugoniot at T = 10 K and T = 300 K. Filled symbols are MD data, open circles are experimental data. MD data was calculated using a monocrystal with the [0001] direction aligned with the shock direction while the experimental data is from a polycrystalline sample. Three wave configurations can be identified from the calculated shock Hugoniot: For particle velocity u_p < 0.8 km/s only an elastic wave is present; Between 0.8 < u_p < 4 km/s a structural phase transformation coexist with a faster and steady elastic wave (not shown); After 3.5 km/s a single overdriven wave is present.

We have also quantified the shock waves calculating the profile of several quantities along the system during the shock propagation. Figures 2(a)-(e) show shock profiles with u_p = 1 km/s calculated after 14.7 ps of initial impact. The particle velocity jumps are the most important indicative of the presence of shock waves and experimentally is the most important measured quantity. Fig. 2(a) show the particle velocity jumps to ~ 730 m/s at the elastic wave front. It keeps that values until the arrive of the transformation wave when the particle velocity goes to 1 km/s. Other thermodynamic quantities, like density, stress, energy and temperature also change abruptly in the shock wave fronts. Fig. 2(b) quantifies the compression of the system.

At the elastic front the density increases from 3.26 g/cm^3 to 3.46 g/cm^3. At the transformation with changes in structure the density reaches 4.1 g/cm^3, which is about 26% higher than the initial value. A useful quantity to distinguish elastic waves from transformation waves is the average movement transverse to the impact. Fig. 2(c) shows the average movement of the particles on the xy plane transverse to the shock direction indicating accurately the threshold for the transformation. At the transformation front the atoms in the average need to displace ~ 1.5 Å. As shown in Fig. 2(c) the xy displacement occurs very quickly in the shock front and is stable along the transformed region. Figs. 2(d)-(f) show yet the stress and energy profile showing the release of the large shear stress created by the elastic wave at the transformation front and the internal energy changes during the elastic and transformation waves.

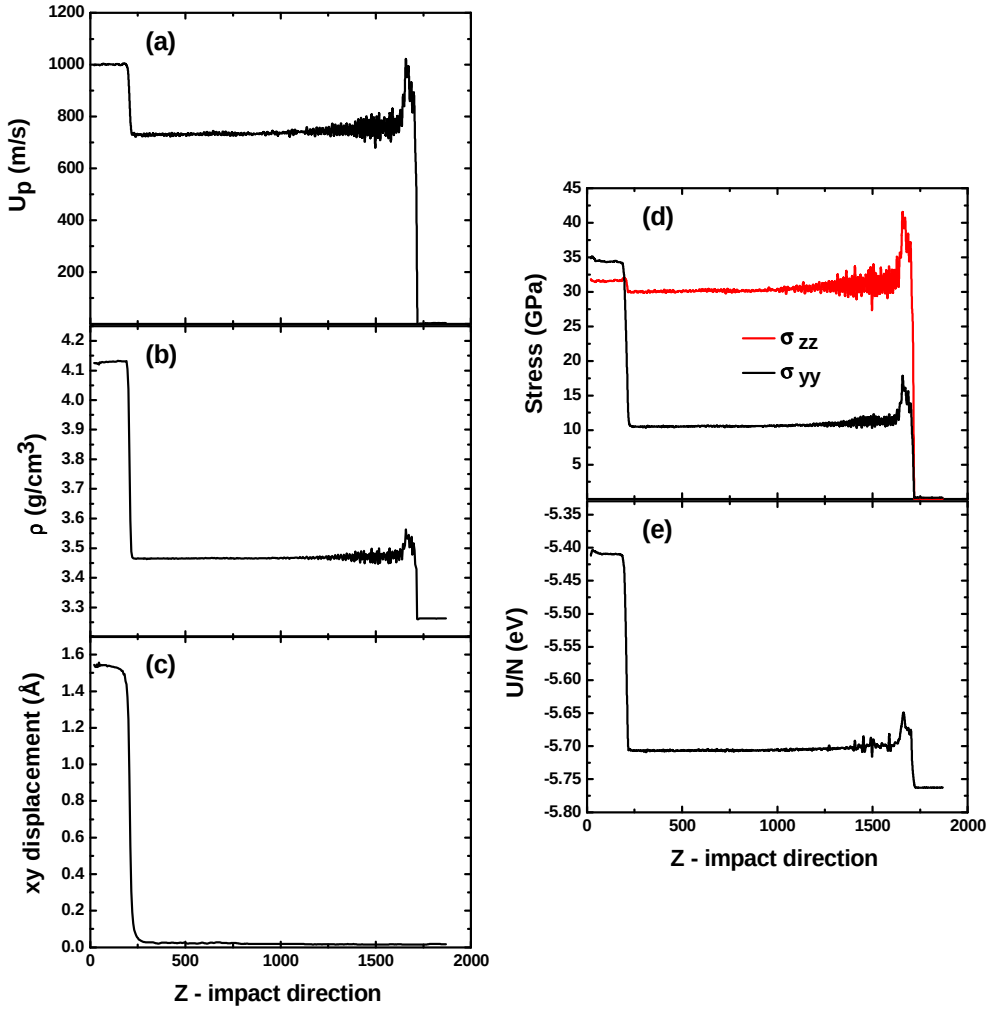

Fig. 2 Shock profiles for impact with u_p = 1 km/s on AlN [0001] direction at 14.7 ps after initial impact. (a) Particle velocities along the whole system. At the elastic shock wave front particles accelerate to ~ 730 m/s, while at the transformation front the velocity reaches the final 1 km/s. (b) Density profile showing the large 26% compression at the transformation. (c) Average movement of particles on the xy plane transverse to the shock direction indicating the threshold for the transformation. (d) Stress profile showing the release of the large shear stress created by the elastic wave at the transformation front. (e) Internal energy changes during the elastic and transformation waves.

The transformation front is sharp and stable and no intermediate region exists. Figures 3(a)-(f) show the atomic structure of the transformation wave.

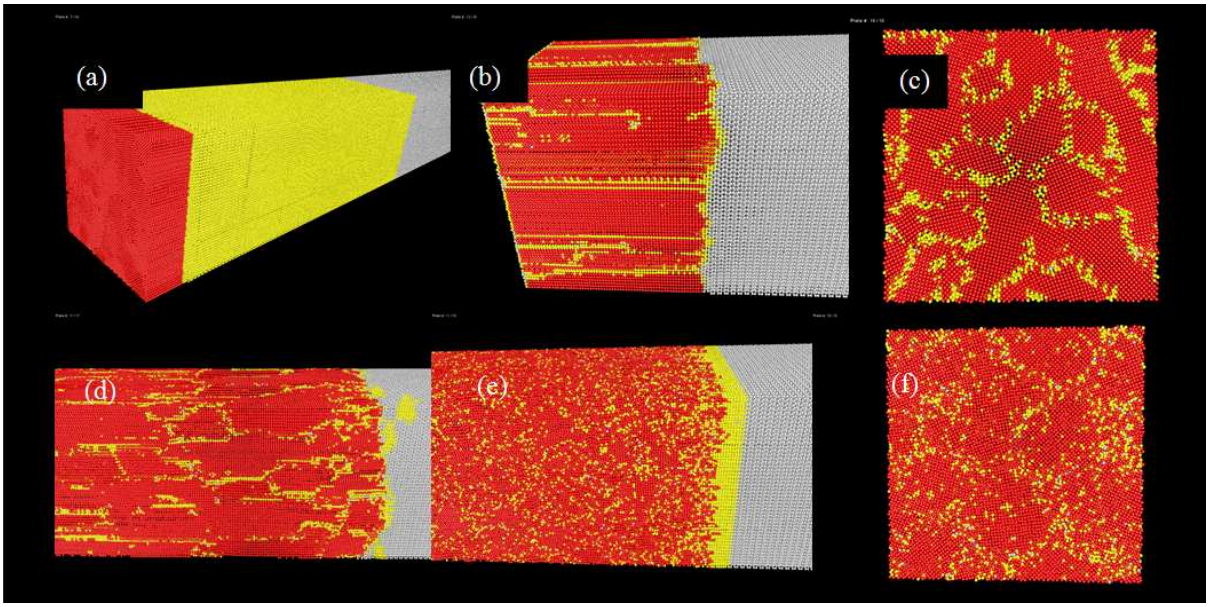

Fig. 3 Shock structure for impacts on AlN [0001] direction. (a)-(b) Shock wave profiles at particle velocity u_p = 1 km/s. (a) Density profile showing uncompressed material (3.26 g/cm^3) in grey, elastically compressed region in yellow (3.46 g/cm^3) and transformed region in red (4.1 g/cm^3). (b) Structure of transformed atoms show grain growing mechanism of transformation propagation. Atoms in (b)-(f) are color coded by the number of neighbors up to 2.5 Å. Grey indicates atoms with 4 neighbors in the original wurtzite crystal. Red indicates atoms with 6 neighbors in the rocksalt transformed crystal. Yellow indicates atoms with 5 neighbors in the front compressed region or in rocksalt grain boundaries. (c) Front face indicates several rocksalt grains nucleated heterogeneously. (d) Transformation at u_p = 2 km/s shows the nucleation of several new grains during the propagation of the transformation wave. (e) Transformation at v_p = 5 km/s shows a sharp transformation wave front with homogeneous nucleation in the shock front, while (f) show healing and growth of grains in the front face of the system.

Figs 3(a)-(b) show the shock profiles at particle velocity u_p = 1 km/s. In Fig. 3(a) the density profile shows an elastic wave (yellow with ~ 3.46 g/cm^3) with a sharp front propagating to the right into the uncompressed material (grey with 3.26 g/cm^3). A slower transformation wave (red with 4.1 g/cm^3) runs behind the elastic wave and drives the system to the rocksalt phase with a density 26 % higher than the original wurtzite. Fig. 3(b) indicates the transformation take place by a grain growing mechanism of nucleated grains at the impact face. Figs 3(b)-(f) show atoms color coded by their coordination number (defined here as the number of neighbors up to 2.5 Å). Grey, red and yellow indicates atoms in the wurtzite phase (coordination 4), rocksalt phase (coordination 6) or compressed wurtzite phase, grain boundary or intermediate phase (coordination 5). Figure 3(c) shows details of the rocksalt grain structure in a plane at 5 Å from the piston surface. Each grain corresponds to a rocksalt nucleation point, indicating that the transformation occurs in a highly heterogeneous nucleation manner. It can be seen that grains have very different sizes and are aligned in three different directions. For u_p up to 2 km/s the final temperature is below 1,000 K and healing of the grains is limited. Grain healing in contrast with metals are very limited until the high particle velocities and high temperatures limit, Fig. 3(f). Increasing the impact velocity and particle velocity change the propagation and the structure of the transformation wave. For u_p = 1 km/s the transformation front is sharp and stable and the mechanism of propagation is based on the growth of the grains nucleated at the face, Fig 3(b). For u_p = 2 km/s, the propagation front is rough and several grains are nucleated as the transformation

front propagates, Fig. 3(d). At u_p = 5 km/s the transformation front become sharp again and the grain growth cannot accompany the fast propagation of the transformation front and there is a high density of nucleation of new rocksalt grains in the front. These grains heal behind the front into larger and energetically favored grains, Fig 3(f). From all the simulations done the calculated Hugoniot indicates the presence of elastic and transformation waves for some u_p in the range 0.8 km/s to 5 km/s. However the results show the transformation wave is reasonably sharp and propagates with no other apparent induced defects.

CONCLUSIONS

In summary we have performed plane shock wave simulations on AlN ceramics with different temperatures and crystallographic directions and large systems of about 4 million atoms. We found three shock response regimes corresponding to three distinguished shock wave profiles. Depending on the particle velocity the shock wave structure is composed by a single elastic wave, a transformation wave preceded by a faster elastic component, or an overdriven wave faster than the sound speed. The crossover between regimes are calculated to be at v_p = 0.8 km/s and v_p = 3.5 km/s, in good agreement with experiments. We have not found an intermediate elastic wave detected experimentally but we believe that variance is related to the difference in crystalline structures used in the experiments and in our simulation. For impact in the [0001] direction the transformation front is sharp and for increasing particle velocity the transformation wave mechanism changes from grain growth (u_p < 2 km/s) (to grain nucleation/growth to multiple grain nucleation (u_p > 4 km/s). The following step is to perform simulations with nanocrystalline structure to complement these results and show the effect of grain size in the shock response of ceramics. It will be particularly interesting to see if a plastic wave is generated in the simulations as a result from grain sliding activity.

REFERENCES

1 Z. Rosenberg, N. S. Brar, and S. J. Bless, Journal of Applied Physics **70**, 167 (1991).
2 D. E. Grady, Journal De Physique Iv **4**, 385 (1994).
3 M. E. Kipp and D. E. Grady, Journal De Physique Iv **4**, 249 (1994).
4 D. P. Dandekar, A. Abbate, and J. Frankel, Journal of Applied Physics **76**, 4077 (1994).
5 D. P. Dandekar, Journal De Physique Iv **4**, 379 (1994).
6 D. E. Grady, Mechanics of Materials **29**, 181 (1998).
7 T. Mashimo, M. Uchino, A. Nakamura, et al., Journal of Applied Physics **86**, 6710 (1999).
8 V. A. Gorelskii, S. A. Zelepugin, and V. F. Tolkachev, Chemical Physics Reports **18**, 2211 (2000).
9 For the functional form of interaction, see J. P. Rino, et al., Phys. Rev. B 70 (2004).
10 P. S. Branicio, R. K. Kalia, A. Nakano, et al., Physical Review Letters **96**, 065502 (2006).
11 P. S. Branicio, R. K. Kalia, A. Nakano, et al., Journal of the Mechanics and Physics of Solids **56**, 1955 (2008).